Transverse Propagation Characteristics and Coherent Effect of Gaussian Beams *

Fei Xiang(向菲)[1], Lin Zhang(张林)[2], Tao Chen(陈涛)[1], Yuan-Hong Zhong(仲元红)[3], Jin Li(李瑾)[4]**

[1]State Grid Chongqing Electric Power Research Institute, Chongqing 401123, China
[2]State Grid Chongqing Electric Power Company, Chongqing 404000, China
[3]School of Microelectronics and Communication Engineering, Chongqing University, Chongqing 400044, China
[4]College of Physics, Chongqing University, Chongqing 401331, China

(Received 10 March 2020)

As an important electromagnetic field in experiment, Gaussian beams have non-vanishing longitudinal electric and magnetic components that generate significant energy fluxes on transverse directions. We focus on the transverse energy flux and derive the theoretical propagation properties. Unlike the longitudinal energy flux, the transverse energy flux has many unique physical behaviors, such as the odd symmetry on propagation, slower decay rate on resonant condition. By means of the characteristics of transverse energy flux, it is feasible to find the suitable regions where the information of coherent lights could be extracted exactly. With the typical laser parameters, we simulate the energy fluxes on receiver surface and analyze the corresponding distribution for the coherent light beams. Especially for coherent lights, the transverse energy flux on the y–z plane with $x = 0$ and x–z plane with $y = 0$, contains pure coherent information. Meanwhile, in the transverse distance $|y| < 2W_0$ (W_0 is the waist radius) and $|x| < W_0/3$ the coherent information could also be extracted appropriately.

PACS: 41.20.Jb, 42.25.Bs, 42.25.Dd DOI: 10.1088/0256-307X/37/6/064101

Gaussian beams, as a typical mode of laser beams, have been widely used and investigated theoretically. Most of the research has focused on the formation of complex Gaussian beams[1–4] and the propagation characteristics in some specific mediums or waveguides.[5–9] Those works are concentrated on the longitudinal field of light beams. Because the longitudinal energy is a benefit for particle acceleration,[10] fluorescent imaging, second-harmonic generation,[11,12] atomic deposition,[13] and Raman spectroscopy.[14] Furthermore, it has been practical to create a pure longitudinal light beam.[15]

However, the transverse field is also important for scientific research because it can enlarge some weak electromagnetic interactions, such as an electromagnetic synchro-resonance system, which could be used to detect very high frequency gravitational waves by extracting the transverse perturbation energy flux.[16–20]

Motivated by the above works, we firstly analyze the energy flux of a standard Gaussian beam in vacuum, and demonstrate the energy flux densities varying with coordinate. Then by generating the coherent Gaussian light beams and calculating the resonant energy flux density numerically, the coherent fringes are obtained on transverse and longitudinal regions. Particularly in the transverse directions, the distribution of energy flux density and the propagation tendency have been changed greatly, which can derive the parameters of the coherent light beams using the information of resonant energy flux. From our results, we have fixed some meaningful regions for distinguishing the coherent light energy and predicted the corresponding decay rate.

The principle of energy flux density.—In theory, a Gaussian beam (GB) is defined as an electromagnetic field whose transverse electric component and the corresponding intensity satisfy Gaussian distribution. Furthermore as a solution to the Helmholtz equation in limited space, a GB can provide a non-vanishing longitudinal electric and magnetic field component except on waist plane. In general, assuming the electromagnetic field propagates along z-axis (cf. Fig. 1(a)), then the transverse electric component can be supposed with standard Gaussian form

$$\tilde{E}_x = \psi = \frac{A}{\sqrt{1+(z/f)^2}} \exp\Big(-\frac{r^2}{W^2}\Big) \cdot \exp\Big[i(kz - \omega t - \tan^{-1}\frac{z}{f} + \frac{kr^2}{2R} + \delta)\Big], \quad (1)$$

and $\tilde{E}_z = 0$, where $r^2 = x^2 + y^2$, $k = 2\pi/\lambda$, $\omega = k^* c$ (c is the speed of light) is the angular frequency of the GB, $f = \pi W_0^2/\lambda$, $W = W_0[1 + (z/f)^2]^{1/2}$ (W_0 is the waist radius of the GB), $R = z + f^2/z$ and δ is the initial phase of GB, t is the time on laboratory coordinate. A is the amplitude of the Gaussian beam, which is determined by the power of laser. According to the Maxwell equations in free space without charge and electric current, $\nabla \cdot \tilde{\boldsymbol{E}} = 0$ and $\tilde{\boldsymbol{B}} = -i\nabla \times \tilde{\boldsymbol{E}}/\omega$, the other electric and magnetic field components could be fixed as follows:

$$\tilde{E}_y = -\int \frac{\partial \tilde{E}_x}{\partial x} = 2x\Big(\frac{1}{W^2} - i\frac{k}{2R}\Big)\int \tilde{E}_x dy, \quad (2)$$

$$\tilde{B}_x = \frac{i}{\omega}\frac{\partial \tilde{E}_y}{\partial z}, \ \tilde{B}_y = -\frac{i}{\omega}\frac{\partial \tilde{E}_x}{\partial z}, \ \tilde{B}_z = \frac{i}{\omega}\Big(\frac{\partial \tilde{E}_x}{\partial y} - \frac{\partial \tilde{E}_y}{\partial x}\Big). \quad (3)$$

*Supported by the National Natural Science Foundation of China (Grant No. 11873001) and the Natural Science Foundation of Chongqing (Grant No. cstc2018jcyjAX0767).
**Corresponding author. Email: cqujinli1983@cqu.edu.cn
© 2020 Chinese Physical Society and IOP Publishing Ltd

From the above electromagnetic field components, the energy flux density of the Gaussian beam in vacuum can be derived as

$$\tilde{\boldsymbol{S}} = \frac{1}{\mu_0}\tilde{\boldsymbol{E}} \times \tilde{\boldsymbol{B}}, \tag{4}$$

where μ_0 is the permeability of vacuum. Generally the energy flux density pulses with time rapidly, so we focus on the average value of $\tilde{S}$ over the time, which could be simplified to[21]

$$\bar{\tilde{\boldsymbol{S}}} = \langle \tilde{\boldsymbol{S}} \rangle = \frac{1}{2\mu_0}\mathrm{Re}(\tilde{\boldsymbol{E}}^* \times \tilde{\boldsymbol{B}}). \tag{5}$$

Then the corresponding components of energy flux density are

$$\begin{aligned}
\bar{\tilde{S}}_x &= \frac{1}{2\mu_0}\mathrm{Re}(\tilde{E}_y^*\tilde{B}_z - \tilde{E}_z^*\tilde{B}_y),\\
\bar{\tilde{S}}_y &= \frac{1}{2\mu_0}\mathrm{Re}(\tilde{E}_z^*\tilde{B}_x - \tilde{E}_x^*\tilde{B}_z),\\
\bar{\tilde{S}}_z &= \frac{1}{2\mu_0}\mathrm{Re}(\tilde{E}_x^*\tilde{B}_y - \tilde{E}_y^*\tilde{B}_x),
\end{aligned} \tag{6}$$

where $\bar{\tilde{S}}_x$ and $\bar{\tilde{S}}_y$ are the transverse energy flux densities, which are much weaker than $\bar{\tilde{S}}_z$ and have many distinctive physical behaviors.

In order to obtain coherent light beams, the Gaussian beam in Fig. 1(b) is split equally into GB_1 and GB_2 while the polarization of GB_2 is rotated vertically, which can be realized by adjusting a zero order half wave plate. In our case, we need to rotate the fast axis of the half wave plate at an angle of 45° with the linear polarization of GB_2. Then combine the two light beams (cf. Fig. 1(b)). Under the coherent condition, the total energy flux density should be the superposition of the individual Gaussian beam energy fluxes and their interaction, which could be

$$\bar{\tilde{\boldsymbol{S}}}_{\mathrm{T}} = \bar{\tilde{\boldsymbol{S}}}_1 + \bar{\tilde{\boldsymbol{S}}}_2 + \bar{\tilde{\boldsymbol{S}}}_{12}, \tag{7}$$

where

$$\bar{\tilde{\boldsymbol{S}}}_{12} = \frac{1}{2\mu_0}\mathrm{Re}(\tilde{\boldsymbol{E}}_1^* \times \tilde{\boldsymbol{B}}_2 + \tilde{\boldsymbol{E}}_2^* \times \tilde{\boldsymbol{B}}_1). \tag{8}$$

Because $\tilde{E}_{1z} = \tilde{E}_{2z} = 0$ and the polarization of GB_2 has been rotated vertically (i.e., $\tilde{E}_{1x} = \tilde{E}_{2y} = \psi$),

$$\begin{aligned}
\tilde{E}_{2x}^*(y,z)|_{x=d} &= \tilde{E}_{1y}^*(x,z)|_{y=d},\\
\tilde{E}_{1y}^*(y,z)|_{x=d} &= \tilde{E}_{2x}^*(x,z)|_{y=d},
\end{aligned} \tag{9}$$

$$\begin{aligned}
\tilde{B}_{2z}(y,z)|_{x=d} &= -\tilde{B}_{1z}(x,z)|_{y=d},\\
\tilde{B}_{1z}(y,z)|_{x=d} &= -\tilde{B}_{2z}(x,z)|_{y=d}.
\end{aligned} \tag{10}$$

The transverse components of the total energy flux density $\bar{\tilde{\boldsymbol{S}}}_{\mathrm{T}}$ are

$$\begin{aligned}
\bar{\tilde{S}}_{\mathrm{T}_x}(y,z)\,|_{x=d} = \frac{1}{2\mu_0}&[\mathrm{Re}(\tilde{E}_{2y}^*\tilde{B}_{2z}) + \mathrm{Re}(\tilde{E}_{1y}^*\tilde{B}_{1z})\\
&+ \mathrm{Re}(\tilde{E}_{2y}^*\tilde{B}_{1z}) + \mathrm{Re}(\tilde{E}_{1y}^*\tilde{B}_{2z})]|_{x=d},
\end{aligned} \tag{11}$$

$$\begin{aligned}
\bar{\tilde{S}}_{\mathrm{T}_y}(x,z)\,|_{y=d} = -\frac{1}{2\mu_0}&[\mathrm{Re}(\tilde{E}_{1x}^*\tilde{B}_{1z}) + \mathrm{Re}(\tilde{E}_{2x}^*\tilde{B}_{2z})\\
&+ \mathrm{Re}(\tilde{E}_{1x}^*\tilde{B}_{2z}) + \mathrm{Re}(\tilde{E}_{2x}^*\tilde{B}_{1z})]|_{y=d},
\end{aligned} \tag{12}$$

Combining Eq. (9)–(12) yields

$$\bar{\tilde{S}}_{\mathrm{T}_x}(y,z)|_{x=d} = \bar{\tilde{S}}_{\mathrm{T}_y}(x,z)|_{y=d}. \tag{13}$$

As the coherent term, $\bar{\tilde{\boldsymbol{S}}}_{12}$ impacts on the transverse energy flux densities significantly, which leads to different distributions, directions of propagation and decay modes. In order to visualize the physical images, the transverse energy flux densities in each case will be numerically simulated in the following.

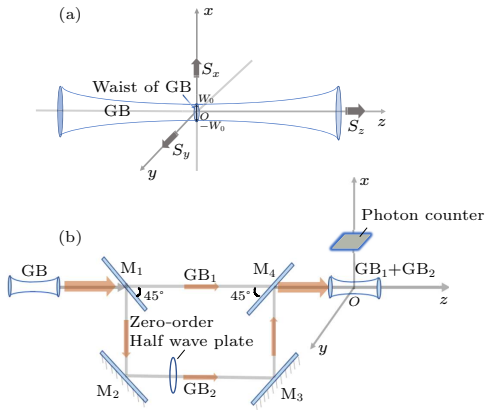

Fig. 1. (a) The diagram of the standard Gaussian beam (GB). (b) The diagram of light path designed to generate two coherent Gaussian beams GB_1 and GB_2, which are obtained by dividing GB equally. Here M_1 and M_4 are half-reflection and half-transmission mirrors, M_2 and M_3 are total reflection mirrors.

The numerical results and discussion.—Unlike a planar electromagnetic wave, a Gaussian beam has non-vanishing transverse energy fluxes. Although the longitudinal energy density plays the major role of energy transmission, the transverse energy is also worth investigating. Especially, when the resonance occurs, the coherent phenomenon in transverse direction is more distinctive than it is in the longitudinal direction.

Considering a standard Gaussian beam expressed by Eq. (1), and all the parameters for the simulation are chosen as follows: (i) For the Gaussian beam, the power is 1 mW, the waist radius $W_0 = 5$ mm, the wavelength is 620 nm, the initial phase is 1.32π. (ii) For the receiver, the receiving surface is assumed as $\Delta s = 5\,\mathrm{mm} \times 5\,\mathrm{mm}$; (iii) On the optical path, the loss of energy on semi spectroscopes M_1, M_4 and the reflection mirrors M_2, M_3 could be neglected.

Once the position of the receiver is fixed, the energy flux density should be a function of the coordi-

nates on the detection surface (i.e., $\bar{\tilde{S}}_x(y,z)$, $\bar{\tilde{S}}_y(x,z)$, $\bar{\tilde{S}}_z(x,y)$). In the experiment, the detector would impact on the original distribution of light intensity if it is immersed in the Gaussian beam, so that we set the receiver located at $2W_0$ away from the coordinate center and simulate the energy flux densities along x, y, z axes. Figure 2 illustrates the simulation of $\bar{\tilde{S}}_x(y,z)$, $\bar{\tilde{S}}_y(x,z)$, $\bar{\tilde{S}}_z(x,y)$ for a single Gaussian beam. It would be found that the transverse energy flux of the Gaussian beam is anti-symmetric to the propagation axis (z-axis), while the longitudinal energy flux is axisymmetric. That is consistent with the theoretical space distribution of the Gaussian beam (i.e., the Gaussian beam will be asymptotically spread as $|z|$ increases).

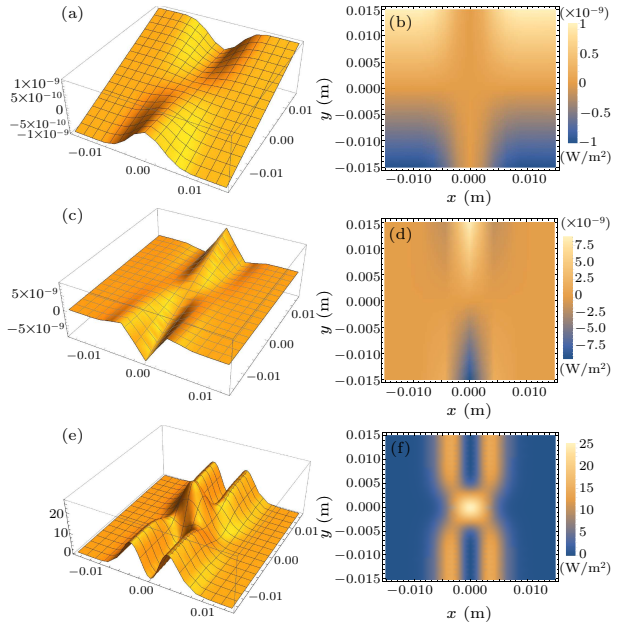

Fig. 2. The 3D figures for (a) $\bar{\tilde{S}}_x$, (c) $\bar{\tilde{S}}_y$, (e) $\bar{\tilde{S}}_z$ of a GB; (b), (d), (f) the cross-sectional plots corresponding to (a), (c), (e), respectively, where the distance between the cross-sectional planes and coordinate center O are $2W_0$. Here the total power of GB laser is chosen to be 1 mW, the waist radius $W_0 = 5$ mm, the wavelength $\lambda = 620$ nm. The negative values of $\bar{\tilde{S}}$ represent that the propagations of the corresponding photons are in the negative directions of the axes.

For the electromagnetic resonant response between two coherent light beams, the coherent fringes will appear due to the interaction between the lights. Similarly, when the coherent Gaussian beams resonantly respond to each other the coherent phenomenon would appear. In Fig. 3, the $\bar{\tilde{S}}_{\text{total}}$ of coherent lights on x, y, z axes have been interfered greatly. It can be noticed that the light and shade stripes distribute alternately in all directions.

In principle, the total power of the outgoing energy flux $\bar{\tilde{S}}_x$ passing through a certain "typical receiving surface" Δs located at x-axis will be the integration of positive values of $\bar{\tilde{S}}_x$ over the Δs at yz plane for $+x$ direction and negative values of $\bar{\tilde{S}}_x$ for $-x$ direction, yielding

$$
\begin{aligned}
P_{+x} &= \frac{1}{2}\int\int_{\Delta s}(\bar{\tilde{S}}_x(y,z) + |\bar{\tilde{S}}_x(y,z)|)dydz,\\
P_{-x} &= \frac{1}{2}\int\int_{\Delta s}(|\bar{\tilde{S}}_x(y,z)| - \bar{\tilde{S}}_x(y,z))dydz,\\
P(x) &= P_{+x} + P_{-x}.
\end{aligned}
\tag{14}
$$

In analogy, the cases in y and z directions could be derived as

$$
\begin{aligned}
P_{+y} &= \frac{1}{2}\int\int_{\Delta s}(\bar{\tilde{S}}_y(x,z) + |\bar{\tilde{S}}_y(x,z)|)dxdz,\\
P_{-y} &= \frac{1}{2}\int\int_{\Delta s}(|\bar{\tilde{S}}_y(x,z)| - \bar{\tilde{S}}_y(x,z))dxdz,\\
P(y) &= P_{+y} + P_{-y},
\end{aligned}
\tag{15}
$$

$$
\begin{aligned}
P_{+z} &= \frac{1}{2}\int\int_{\Delta s}(\bar{\tilde{S}}_z(x,y) + |\bar{\tilde{S}}_z(x,y)|)dxdy,\\
P_{-z} &= \frac{1}{2}\int\int_{\Delta s}(|\bar{\tilde{S}}_z(x,y)| - \bar{\tilde{S}}_z(x,y))dxdz,\\
P(z) &= P_{+z} + P_{-z}.
\end{aligned}
\tag{16}
$$

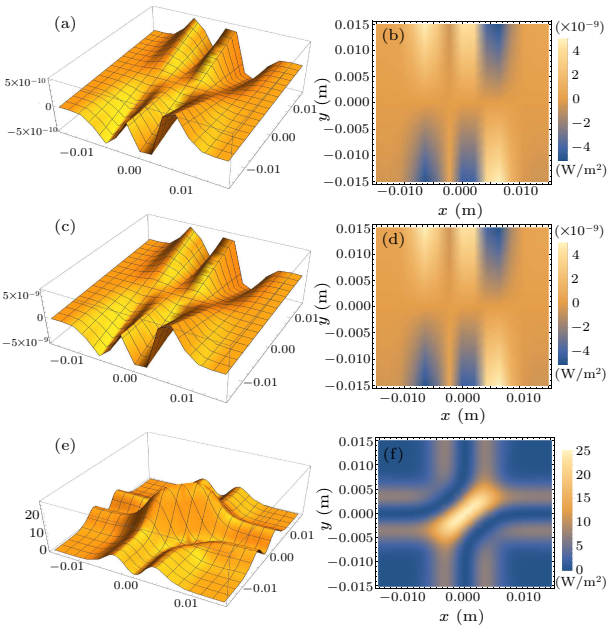

Fig. 3. The 3D figures for (a) $\bar{\tilde{S}}_x$, (c) $\bar{\tilde{S}}_y$, (e) $\bar{\tilde{S}}_z$ after resonant interaction between two resonant GBs; (b), (d), (f) the cross-sectional plots corresponding to (a), (c), (e), respectively, where the distance between the cross-sectional planes and coordinate center O are $2W_0$. Here the total power of GB laser is chosen to be 1 mW, the waist radius $W_0 = 5$ mm, the wavelength $\lambda = 620$ nm. The negative values of $\bar{\tilde{S}}$ represent that the propagations of the corresponding photons are the negative directions of the axes.

To further investigate the properties of energy flux densities, we can set a photon counter with receiving area facing the specific transverse energy flux in experiment. As a camera, the photon counter is able to capture the 2D energy distribution on each point, then the specific transverse energy flux densities can be recorded and separated. Unlike the light intensity, the

energy flux density describes not only light intensity on unit area but also the direction of light propagation on unit area. Thus their difference is that the interference fringes in the negative direction have bright light intensity, but would have dark fringes of energy flux density. For example, in the case of Fig. 3(b), the photon counter should be set on the $+x$ axis as shown in Fig. 1(b), then in the counter we can find that there are bright fringes where maximal photons appear on $+x$ axis, the areas of dark fringes where maximal photons go toward to $-x$ axis no longer reach the receiving surface so that they would not be recorded in the counter. That is the reason for choosing energy flux densities instead of light intensity to investigate interference phenomenon.

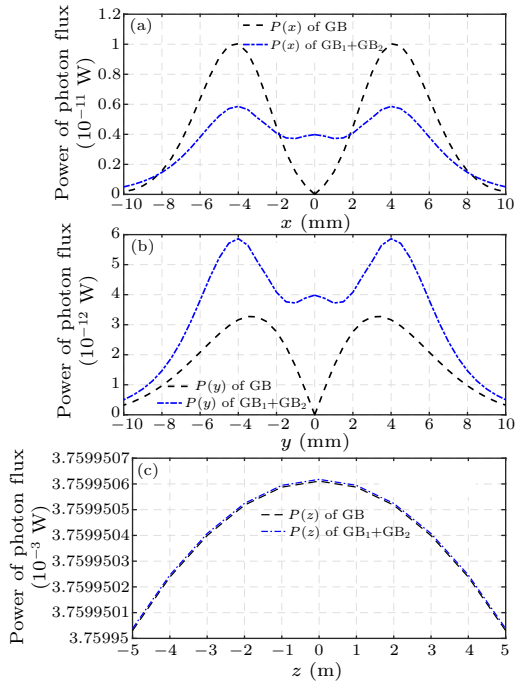

Fig. 4. The total power of the outgoing energy flux (a) $\bar{\bar{S}}_x$, (b) $\bar{\bar{S}}_y$, (c) $\bar{\bar{S}}_z$ passing through a certain "typical receiving surface" Δs located at x, y, z axes respectively. In each subplot, the blue dotted line is the energy flux generated after resonance, the black dashed line means the energy flux generated by a single GB.

In our simulation, without loss of generality we shall consider the energy flux propagating along the directions of the x, y, and z axes. Figure 4 shows the comparison of $P(x)$, $P(y)$, and $P(z)$ generated by a single GB and two coherent GBs respectively, which indicate that the transverse energy fluxes have different decay modes after coherent interaction but the decay speed and mode of longitudinal energy flux is unchanged. That characteristic provides some possible detection regions where the coherent behavior could be configured suitably, with the given systematic parameters we can extract the coherent energy from the background field within $W_0 < |y| < 2W_0$, which can be called the effective region. The reasons for fixing the range are: (1) the receiver should not be immersed in the light field of the original Gaussian beam, so it should be $>W_0$, (2) the coherent energy flux (blue dotted line in Fig. 4) should be larger than the energy flux without coherence (black dashed line in Fig. 4). In our work, the waist $W_0 = 5$ mm. Therefore only when the photon counter located on y axis (Fig. 4(b)), is it possible to find the range where the coherent energy flux is larger than the energy flux without coherence beyond the waist. Thus it is $W_0 < |y| < 2W_0$, beyond $2W_0$ they approach to be the same. From Figs. 2–4, we can find that the energy flux distributions have great changes after coherence, especially on transverse directions. That implies that on the transverse direction, electromagnetic interaction is also important, moreover it has more distinct properties of energy flux and power distribution than those on longitudinal direction. These properties are helpful for us to extract coherent information. For example, given the physical parameters of one coherent light GB$_1$, the EM components of the other GB$_2$ could be derived from the coherent fringes in the effective region where the coherent energy flux is larger than the energy flux without coherence. Therefore it is feasible to extract the resonance information of the Gaussian beam by screening the transverse energy flux.

Conclusion and Remarks.—Taking a standard Gaussian beam as our target light beam, we analyze the distributions of energy flux densities of a single light and the coherent lights. The transverse light intensity is weak but it has unique energy flux distribution and propagation. For a single Gaussian beam, the results illustrate that the energy flux of the Gaussian beam transmits along the propagation direction, meanwhile it spreads out in the $+z$ and $-z$ directions. For the coherent Gaussian beams, the resonance impacts on the energy flux significantly and changes the irradiance surface of the final beam. Furthermore, the power of transverse energy has been re-configured in the transverse directions, while the longitudinal energy has almost the same transmission mode as before. These properties provide a possibility to distinguish the effect of resonant interaction in some suitable regions.

The resonance information mentioned above mainly focus on the physical parameters of the coherent EM field on each light path. The reason for extracting it is that, when only one EM field (such as GB$_1$) is determined, the physical parameters of the other one (such as the amplitude of GB$_2$) unknown in advance would be derived from extracting the coherent energy flux or coherent power in the effective regions. In addition, applying this approach is possible to detect gravitational waves (GWs) in the coherent frequency band. Because the interaction of GWs and EM would result in the equivalent EM field as GB$_2$, which includes the information of GWs (such as strength and frequency).

The above results are obtained under a specific laser system. In fact, we can adjust the corresponding

parameters to observe the relationship between energy flux and laser properties. In fact, the Gaussian beam will resonate with other types of light beam to obtain similar transverse distribution of energy transmission, such as plane wave, other varieties of Gaussian beams. In this way, some correlation information can be extracted by analyzing the distribution characteristics of transverse photon flux.

References

[1] Gori F, Guattari G and Padovani C 1987 *Opt. Commun.* **64** 491
[2] Wen J J and Breazeale M A 1988 *J. Acoust. Soc. Am.* **83** 1752
[3] Wang H Y, Peng, X F and Liu L 2019 *Opt. Lett.* **44** 3709
[4] Liu D J, Zhong H Y, Wang G Q, Yin H M and Wang Y C 2020 *Opt. Laser Technol.* **124** 106003
[5] Jin L 2020 *Phys. Scr.* **95** 035502
[6] Liu H L, Ralston J and Yin P M 2020 *Math. Comput.* **89** 675
[7] Yang Z K, Lin X L, Zhang H, Xu Y T, Jin L, Zou Y G and Ma X H 2020 *Opt. Lasers Eng.* **126** 105899
[8] Worku N G and Gross H 2019 *J. Opt. Soc. Am. A* **36** 859
[9] Guo L, Tang Z L and Wan W 2014 *Optik* **125** 5542
[10] Wang J F, Zhang D Q, Huang S J, Wu X Y and Wang P X 2018 *Appl. Phys. B* **124** 204
[11] Sukhdeep K, Sharma A K and Salih H A 2009 *Phys. Plasmas* **16** 042509
[12] Nadeem A A and Zubairy M S 1986 *Opt. Commun.* **59** 385
[13] Chen J, Liu J, Zhu L, Deng X, Cheng X B and Li T B 2020 *Chin. Phys. B* **29** 020601
[14] Cormack I G, Mazilu M and Dholakia K 2007 *Appl. Phys. Lett.* **91** 023903
[15] Wang H F, Shi L P, Lukyanchuk B, Sheppard C and Chong C T 2008 *Nat. Photon.* **2** 501
[16] Li J, Lin K, Li F Y and Zhong Y H 2011 *Gen. Relativ. Gravit.* **43** 2209
[17] Wen H, Li F Y and Fang Z Y 2014 *Phys. Rev. D* **89** 104025
[18] Wen H, Li F Y, Fang Z Y and Beckwith A 2014 *Eur. Phys. J. C* **74** 2998
[19] Wang L L and Li J 2018 *Gravitation Cosmol.* **24** 22
[20] Li J, Li F Y and Zhong Y H 2009 *Chin. Phys. B* **18** 0922
[21] Walter G 2018 *Classical Electrodynamics* (Beijing: World Publishing Corporation)